

$\pi^+\pi^-$ Emission from Coherent ρ^0 Propagation in Nuclei

Swapan Das

*Nuclear Physics Division, Bhabha Atomic Research Centre
Mumbai-400085, India*

Abstract

Cross sections for the $\pi^+\pi^-$ events arising due to the decay of ρ^0 meson have been calculated. This rho meson is considered to produce coherently in the (p, p') reaction on a nucleus. The distorted wave functions for the continuum particles and the rho meson propagator are described by the eikonal form. The sensitivity of the cross section on the pion emission angle as well as on the beam energy has been investigated. The cross sections for the ρ^0 decaying inside and outside the nucleus are compared. In addition, the coherent and incoherent contributions to the cross section due to ρ^0 inside and outside decay amplitudes are presented. The initial and final state interactions for this reaction have been studied. The nuclear medium effect on the ρ^0 propagation through the nucleus is also explored.

1 Introduction

The hadron parameters for vector mesons embedded in the nucleus may differ significantly from their free space values due to the interaction taken place between the vector mesons and the other nuclear particles present in the nucleus. Therefore, the study on the in-medium properties of vector mesons can offer valuable informations about the vector meson dynamics in a nucleus. In compressed [$\rho \approx (3 - 5)\rho_0$] and/or hot [$\sim (150 - 200)$ MeV] nuclei, the medium effect on the vector meson could be drastic. In fact, large medium effect on the rho meson is believed to be seen in the enhanced dilepton yield in CERES and HELIOS ultra-relativistic heavy ion collision data [1] taken in CERN-SPS. Theoretically, these data are found to be compatible if the ρ mass is reduced drastically, i.e., by $\sim 300 - 400$ MeV [2]. In contrast to this, these data are also reproduced successfully by calculations [3] which incorporate the hadronic interaction for the rho meson with the surrounding nuclear particles. Recent analysis on the $\pi^+\pi^-$ pairs, in the STAR experiment at BNL RHIC, showed a decrease in ρ mass in the peripheral Au + Au collisions [4].

There exist some model calculations which envisage the reduction of vector meson mass in the nuclear medium. For example, the scaling hypothesis due to Brown and Rho [5] shows that the mass of vector meson in a nucleus should drop, since the pion weak decay constant does. The QCD sum rule calculation done by Hatsuda

and Lee [6] shows that the reduction in the vector meson mass increases with the nuclear density. This finding is also corroborated by the vector dominance model (VDM) calculation due to Asakawa et al., [7]. The quark meson (QM) coupling model calculation done by Saito et al., [8] shows that the mass of ρ meson in the ^{12}C nucleus is reduced by 50 MeV. Beside these, the manybody calculations show that the spectral function for the rho meson in the nuclear medium gets modified significantly due to its interaction with the nucleon and resonances. In one of these calculations, Frimann et al., [9] have shown that the p wave ρN scattering [via $N(1720)$ and $\Delta(1905)$ resonances] reduces the mass of rho meson, and this reduction is significant in high baryon density. Peters et al., [10] have extended this calculations by incorporating all four starred s and p wave resonances. Their calculations show a strong influence of the s wave resonances on the ρ spectral function, specifically in the static limit. The density dependent two pion self-energy calculation due to Herrmann et al., [11] shows an enhancement in the in-medium ρ width, but they have not found, unlike others, any significant change in the in-medium ρ mass. The recent developments in this field are illustrated in the Ref. [12].

To look for the in-medium properties of vector mesons in a normal nucleus, experimental programmes are there at various centers around the world. For example, it has been proposed to measure the photo production of vector meson in the nucleus at TJNAF through the e^+e^- radiation [13], and at 1.3 GeV Tokyo Electron Synchrotron (INS) through the $\pi^+\pi^-$ emission [14]. Recently, CBELSA/TAPS Collaboration at ELSA [15] had found the medium modification on the omega meson in ^{93}Nb nucleus. The KEK-PS E325 collaboration at KEK [16] had measured the e^+e^- yield in the $p+A$ reaction at 12 GeV, and they have reported an enhancement in this yield in the region of $0.6 \geq m_{e^+e^-} \leq 0.77$ GeV/ c^2 due to modified ρ meson in nuclei. Another experiment [17] in this collaboration (which investigates the medium effect on ϕ meson) is in progress. There also exist experimental programmes at GSI-SIS [18] (HADE collaboration) as well as at Spring-8 RCNP [19], which are dedicated to explore the hadron parameters for vector mesons in the normal nucleus. Therefore, the overall view for the medium modification on vector mesons is expected in near future.

There also exist several calculations showing the medium effect on vector mesons in the normal nucleus. Eletsky et al., [20] and Kondratyuk et al., [21] relate the effective mass and width for the rho meson in a nucleus to the ρ nucleon scattering amplitude $f_{\rho N}$ and nuclear density. In their calculations, it has been shown that the mass of the rho meson in a normal nucleus increases with its energy. In the static limit, the ρ mass is below its free space value, where as it exceeds 770 MeV at higher energies [21]. Effenberger et al., have studied the e^+e^- production from the gamma [22] and pion [23] induced nuclear reactions at GeV energies in the framework of

semiclassical Boltzmann-Uehling-Uhlenbeck (BUU) transport model. Their study shows that the medium modification on vector mesons enhances the dilepton yields in the e^+e^- invariant mass region below 770 MeV. The Intranuclear Cascade (INC) model calculation due to Golubeva et al., [24] also supports this conclusion. Several studies [25] show the width of ϕ meson in a nucleus increases significantly, where as the mass-shift for it is insignificant.

Another way to explore the ρ dynamics in a normal nucleus could be through the coherent ρ^0 production in the (p, p') reaction. The coherent meson production process had been used earlier to unveil many interesting aspects in the nuclear dynamics. For example, the pion and delta dynamics in a nucleus were investigated sometime back through the coherent photo- and electro-production of pion in the Δ excitation region [26, 27, 28]. In this energy region, the measurements had been done, in the recent past, on the coherent π^+ production in the charge exchange reactions [29]. These reactions offer valuable informations [30], which are complementary to those obtained from the scattering of real pion on a nucleus [26, 27].

For the coherent ρ^0 emission in the (p, p') reaction, it is visualized that the beam proton emits rho meson. This rho meson, of course, is a virtual particle, since the four-momentum carried by it is constrained by the dispersion relation obeyed by protons. It is the nucleus which scatters this ρ^0 meson coherently and brings it on-shell. Kinematically, this process is possible because the recoiling nucleus, as a whole, can adjust the momentum to put the virtual rho meson on its mass-shell. For simplicity, we restrict the propagation of the coherent ρ^0 meson to the forward direction only. This rho meson, after traveling a certain distance, decays into π^+ and π^- in the final state. Naturally, the ρ^0 dynamics in this reaction can be manifested from these $\pi^+\pi^-$ events. Therefore, the coherent rho meson production process can be thought as a pertinent probe to acquire the knowledge about the ρ nucleus interaction.

The energy transfer $E_p - E_{p'}$ distribution spectra have been calculated for the $(p, p'[\pi^+\pi^-])$ reaction on various nuclei. According to the model presented here, the $\pi^+\pi^-$ in the final state arise due to the decay of coherent ρ^0 meson, propagating through a nucleus. This calculation is based on Glauber approach for the nuclear effect. Where the distorted wave functions for the continuum particles (i.e., p , p' , π^+ and π^-) and the ρ^0 propagator have been described by the eikonal form. The potential required to generate these quantities is constructed by using “ $t\rho$ ” approximation. In this study, the dependence of the cross section on the pion emission angle as well as on the beam energy is presented. The cross sections for the rho meson decaying inside and outside the nucleus are compared. Along with this, the coherent and incoherent contributions to the cross section due to the inside and outside decay for the rho meson are also studied. The initial and final state interactions

for this reaction are investigated. In addition, the medium effect on the rho meson propagating through the nucleus is explored.

We write the formalism in Sec. 2 for the coherent rho meson production in the (p, p') reaction and its decay into π^+ and π^- in the final state. The results and discussion for this reaction are illustrated in Sec. 3. Conclusions obtained from this study have been presented in Sec. 4.

2 Formalism

The formalism for the $\pi^+\pi^-$ emission from the rho meson, propagating through a nucleus, has been developed here. This rho meson is produced coherently in the (p, p') reaction on a nucleus. The T -matrix T_{fi} for this reaction consists of production, propagation, and decay (into two pions) for the rho meson, i.e.,

$$T_{fi} = \int \int d\mathbf{r} d\mathbf{r}' \chi^{(-)*}(\mathbf{k}_{\pi^+}, \mathbf{r}') \chi^{(-)*}(\mathbf{k}_{\pi^-}, \mathbf{r}') \Gamma_{\rho\pi\pi} S_\rho(\mathbf{r}' - \mathbf{r}) \Psi_{\rho^0}(\mathbf{r}). \quad (1)$$

The factor $\Psi_{\rho^0}(\mathbf{r})$ in the above equation represents the ρ^0 production amplitude due to (p, p') reaction. It is given by

$$\Psi_{\rho^0}(\mathbf{r}) = \Pi_\rho(q_0, \mathbf{r}) G_\rho(q^2) \chi^{(-)*}(\mathbf{k}_{p'}, \mathbf{r}) \Gamma_{\rho NN} \chi^{(+)}(\mathbf{k}_p, \mathbf{r}), \quad (2)$$

where $\Pi_\rho(q_0, \mathbf{r}) [= 2q_0 V_{O\rho}(\mathbf{r})]$ denotes the self-energy for the rho meson, arising due to ρ nucleus optical potential $V_{O\rho}(\mathbf{r})$. This potential describes the elastic scattering of the virtual rho meson to its real state. $q_0 (= E_p - E_{p'})$ is the energy carried out by the virtual rho meson. $\tilde{G}_\rho(q^2)$ represents the propagator for the virtual rho meson emitted at the $\rho^0 pp'$ vertex: $\tilde{G}_\rho(q^2) = -\frac{1}{m_\rho^2 - q^2}$. Here, m_ρ (~ 770 MeV) and $q (= k_p - k_{p'})$ are the mass and the four momentum respectively for the rho meson. χ s, given in Eq. (2), denote the distorted wave functions for protons. In eikonal approximation, they can be written as

$$\chi^{(+)}(\mathbf{k}_p, \mathbf{r}) = e^{i\mathbf{k}_p \cdot \mathbf{r}} \exp \left[-\frac{i}{v_p} \int_{-\infty}^z dz' V_{Op}(\mathbf{b}, z') \right],$$

and

$$\chi^{(-)*}(\mathbf{k}_{p'}, \mathbf{r}) = e^{-i\mathbf{k}_{p'} \cdot \mathbf{r}} \exp \left[-\frac{i}{v_{p'}} \int_z^\infty dz' V_{Op'}(\mathbf{b}, z') \right]. \quad (3)$$

$\Gamma_{\rho NN}$, in Eq. (2), is the vertex function at the $\rho^0 pp'$ vertex. It describes the emission of virtual ρ^0 at this vertex. The Lagrangian, describing the interaction at the ρNN vertex, is given by

$$\mathcal{L}_{\rho NN} = -g_V F(q^2) \bar{N} [\gamma^\mu - i \frac{\kappa}{2m_N} \sigma^{\mu\nu} q_\nu] \tau \cdot \rho_\mu N, \quad (4)$$

with $g_V = 2.6$ and $\kappa = 6.1$ [26]. $F(q^2)$ represents the form factor at the ρNN vertex: $F(q^2) = \frac{\Lambda^2 - m_\rho^2}{\Lambda^2 - q^2}$, with $\Lambda = 1.3$ GeV/c [31]. The quantities m_ρ and q are already defined below the Eq. (2).

The factor $S_\rho(\mathbf{r}' - \mathbf{r})$, appearing in Eq. (1), describes the propagation for the real ρ^0 meson from the position \mathbf{r} to another position \mathbf{r}' . Which, in the present work, has been restricted to the forward direction only. Therefore, $S_\rho(\mathbf{r}' - \mathbf{r})$ can be expressed in the eikonal form as

$$S_\rho(\mathbf{r}' - \mathbf{r}) = \delta(\mathbf{b}' - \mathbf{b})\Theta(z' - z)e^{i\mathbf{k}_\rho \cdot (\mathbf{r}' - \mathbf{r})} D_{\mathbf{k}_\rho}(\mathbf{b}, z', z), \quad (5)$$

where $D_{\mathbf{k}_\rho}(\mathbf{b}, z', z)$ describes the nuclear medium effect on the ρ propagation through a nucleus. It is given by

$$D_{\mathbf{k}_\rho}(\mathbf{b}, z', z) = -\frac{i}{2k_\rho} \exp \left[\frac{i}{2k_\rho} \int_z^{z'} dz'' \{ \tilde{G}_{0\rho}^{-1}(m) - 2E_\rho V_{O\rho}(\mathbf{b}, z'') \} \right]. \quad (6)$$

In this equation, k_ρ is the momentum for the forward going rho meson. $V_{O\rho}(\mathbf{b}, z'')$, as mentioned earlier, represents the optical potential for the rho meson. $\tilde{G}_{0\rho}^{-1}(m)$ represents the inverse of the free rho meson (on-shell) propagator. It is given by

$$\tilde{G}_{0\rho}^{-1}(m) = m^2 - m_\rho^2 + im_\rho \Gamma_\rho(m); \quad \Gamma_\rho(m) = \Gamma_\rho(m_\rho) \left(\frac{m_\rho}{m} \right) \left[\frac{k(m^2)}{k(m_\rho^2)} \right]^3, \quad (7)$$

with $m_\rho \approx 770$ MeV and $\Gamma_\rho(m_\rho) \sim 150$ MeV, for $\rho^0 \rightarrow \pi^+\pi^-$ in the free state. $k(m^2)$ is the momentum for pion in the rest frame of decaying rho meson of mass m .

$\Gamma_{\rho\pi\pi}$, in Eq. (1), describes the vertex function for the ρ^0 meson decaying into $\pi^+\pi^-$ in the final state. It is governed by the Lagrangian:

$$\mathcal{L}_{\rho\pi\pi} = f_{\rho\pi\pi} \rho^\mu \cdot (\pi \times \partial_\mu \pi), \quad (8)$$

with $f_{\rho\pi\pi} \approx 6.1$ [26, 32].

The distorted wave functions χ s, in Eq. (1), for pions in the final state have been described by the eikonal form, i.e.,

$$\chi^{(-)*}(\mathbf{k}_{\pi^+}, \mathbf{r}') \chi^{(-)*}(\mathbf{k}_{\pi^-}, \mathbf{r}') = e^{-i(\mathbf{k}_{\pi^+} + \mathbf{k}_{\pi^-}) \cdot \mathbf{r}'} D_{\mathbf{k}_\pi}(\mathbf{b}', z'). \quad (9)$$

In this equation, $D_{\mathbf{k}_\pi}(\mathbf{b}', z')$ represents the distortion occurring due to the elastic scattering of pions by the recoiling nucleus. It is given by

$$D_{\mathbf{k}_\pi}(\mathbf{b}', z') = \exp \left[-i \int_{z'}^\infty dz'' \left\{ \frac{V_{O\pi^+}(\mathbf{b}', z'')}{v_{\pi^+}} + \frac{V_{O\pi^-}(\mathbf{b}', z'')}{v_{\pi^-}} \right\} \right], \quad (10)$$

where v_{π^\pm} is the velocity of π^\pm , and $V_{O\pi^\pm}(\mathbf{b}', z')$ denotes the optical potential for the π^\pm scattering on a nucleus.

The T -matrix T_{fi} , given in Eq. (1), can be factorized into interaction and structure parts. The interaction part contains the production and decay vertex functions (i.e., $\Gamma_{\rho NN}\Gamma_{\rho\pi\pi}$) for the rho meson. The structure part carries the information about the medium effect on the rho meson. The later, using Eqs. (1), (5) and (9), can be written as

$$F = \int d\mathbf{r} D_{\pi\rho}(\mathbf{k}_\pi, \mathbf{k}_\rho; \mathbf{b}, z) e^{-i\mathbf{k}_\rho \cdot \mathbf{r}} \Pi_\rho(q_0, \mathbf{r}) \tilde{G}_\rho(q^2) \chi^{(-)*}(\mathbf{k}_{\mathbf{p}'}, \mathbf{r}) \chi^{(+)}(\mathbf{k}_{\mathbf{p}}, \mathbf{r}), \quad (11)$$

with $\mathbf{k}_\rho = \mathbf{k}_{\pi^+} + \mathbf{k}_{\pi^-}$. The symbol $D_{\pi\rho}(\mathbf{k}_\pi, \mathbf{k}_\rho; \mathbf{b}, z)$ appearing in this equation stands for

$$D_{\pi\rho}(\mathbf{k}_\pi, \mathbf{k}_\rho; \mathbf{b}, z) = \int_z^\infty dz' D_{\mathbf{k}_\pi}(\mathbf{b}, z') D_{\mathbf{k}_\rho}(\mathbf{b}, z', z), \quad (12)$$

where $D_{\mathbf{k}_\rho}(\mathbf{b}, z', z)$ and $D_{\mathbf{k}_\pi}(\mathbf{b}, z')$ are defined in Eqs. (6) and (10) respectively. The above equation describes the dynamics for the pi and rho mesons in the nucleus.

The rho meson, due to its short life time ($\sim 10^{-23}$ sec), can decay inside as well as outside the nucleus, depending upon its velocity and the size of the nucleus. Indeed, the physical quantity which determines this decay probability is the effective decay length: $\lambda^* = v/\Gamma^*$. Where v and Γ^* describe the velocity and the effective decay width respectively for the rho meson in a nucleus. This decay length λ^* controls over the attenuation for the in-medium ρ propagation. While the rho meson propagates a distance $L(\mathbf{b}, z) [= \sqrt{R^2 - b^2} - z]$ from the production point z to the surface of a nucleus of radius R , it gets attenuated by a factor $\exp[-L(b, z)/\lambda^*]$. To investigate the inside and outside decay probabilities more transparently, $D_{\pi\rho}(\mathbf{k}_\pi, \mathbf{k}_\rho; \mathbf{b}, z)$ in Eq. (12) is splitted into two parts, i.e.,

$$D_{\pi\rho}(\mathbf{k}_\pi, \mathbf{k}_\rho; \mathbf{b}, z) = D_{\pi\rho}^{in}(\mathbf{k}_\pi, \mathbf{k}_\rho; \mathbf{b}, z) + D_{\pi\rho}^{out}(\mathbf{k}_\pi, \mathbf{k}_\rho; \mathbf{b}, z). \quad (13)$$

In this equation, $D_{\pi\rho}^{in}(\mathbf{k}_\pi, \mathbf{k}_\rho; \mathbf{b}, z)$ and $D_{\pi\rho}^{out}(\mathbf{k}_\pi, \mathbf{k}_\rho; \mathbf{b}, z)$ correspond to the probability for the rho meson decaying inside and outside the nucleus respectively. They are given by

$$D_{\pi\rho}^{in}(\mathbf{k}_\pi, \mathbf{k}_\rho; \mathbf{b}, z) = \int_z^{\sqrt{R^2 - b^2}} dz' D_{\mathbf{k}_\pi}(\mathbf{b}, z') D_{\mathbf{k}_\rho}(\mathbf{b}, z', z), \quad (14)$$

and

$$D_{\pi\rho}^{out}(\mathbf{k}_\pi, \mathbf{k}_\rho; \mathbf{b}, z) = \int_{\sqrt{R^2 - b^2}}^\infty dz' D_{\mathbf{k}_\pi}(\mathbf{b}, z') D_{\mathbf{k}_\rho}(\mathbf{b}, z', z). \quad (15)$$

In the later equation, i.e., in Eq. (15), $D_{\mathbf{k}_\pi}(\mathbf{b}, z')$ goes to unity, and $D_{\mathbf{k}_\rho}(\mathbf{b}, z', z)$ reduces to $-\frac{i}{2k_\rho} \exp[\frac{i}{2k_\rho} \tilde{G}_{0\rho}^{-1}(m_\rho)(z' - z)]$.

For the $\pi^+\pi^-$ emission in the (p, p') reaction on a nucleus, the differential cross section, $\frac{d\sigma}{dE_{p'}d\Omega_{p'}dE_{\pi^+}d\Omega_{\pi^+}dE_{\pi^-}d\Omega_{\pi^-}}$, for the energy transfer transfer $E_p - E_{p'}$ distribution can be written as

$$\frac{d\sigma}{dE_{p'}d\Omega_{p'}dE_{\pi^+}d\Omega_{\pi^+}dE_{\pi^-}d\Omega_{\pi^-}} = \frac{\pi^3}{(2\pi)^{11}} \frac{m_p^2 k_{p'} k_{\pi^+} k_{\pi^-}}{k_p} \langle |T_{fi}|^2 \rangle. \quad (16)$$

The annular bracket around the $|T_{fi}|^2$ represents the average over the spin orientations of the particles in the initial state and the summation over the spin orientations of the particles in the final state.

3 Results and Discussion

To calculate the T -matrix T_{fi} , given in Eq. (1), it is necessary to evaluate the wave functions for protons in Eq. (3) and pions in Eq. (9), as well as the propagator for the rho meson in Eq. (5). The important ingredient required to generate these quantities is the optical potential for the respective particles. This potential, in the present work, has been estimated using “ $t\rho$ ” approximation. According to it, the optical potential $V_{OX}(\mathbf{r})$ for a particle X scattered off by a nucleus can be expressed [33] as

$$V_{OX}(\mathbf{r}) = -\frac{v_X}{2}(i + \alpha_{XN})\sigma_t^{XN}\varrho(\mathbf{r}). \quad (17)$$

α_{XN} appearing in this equation denotes the ratio: $Ref_{XN}(0)/Imf_{XN}(0)$. Here, $f_{XN}(0)$ is the particle nucleon ($X - N$) scattering amplitude at the forward direction. σ_t^{XN} represents the total scattering cross section. $\varrho(\mathbf{r})$ denotes the spatial distribution for the nuclear density, usually approximated by the charge density distribution for the nucleus. The present work deals with ^{12}C and ^{208}Pb nuclei only. Therefore, the form of $\varrho(\mathbf{r})$ for these nuclei, as extracted from the electron scattering data [34], is given by

$$^{12}\text{C} : \quad \varrho(\mathbf{r}) = \varrho_0[1 + w(r/c)^2]e^{-(r/c)^2}; \quad w = 1.247, \quad c = 1.649 \text{ fm}. \quad (18)$$

$$^{208}\text{Pb} : \quad \varrho(\mathbf{r}) = \varrho_0 \frac{1 + w(r/c)^2}{1 + \exp(\frac{r^2 - c^2}{a^2})}; \quad w = 0.3379, \quad c = 6.3032 \text{ fm}, \quad a = 2.8882 \text{ fm}. \quad (19)$$

These densities are normalized to the mass numbers of the corresponding nuclei.

To evaluate the proton nucleus optical potential $V_{Op}(\mathbf{r})$ in Eq. (17), the energy dependent measured values for the proton nucleon scattering parameters, i.e., α_{pN} and σ_t^{pN} , [35, 36] have been used. Similarly, $\alpha_{\pi^\pm N}$ and $\sigma_t^{\pi^\pm N}$ are used as input quantities in Eq. (17) to generate the π^\pm nucleus optical potential $V_{O\pi^\pm}(\mathbf{r})$. The

data for $\sigma_t^{\pi^\pm p}$ exist for a wide range of energy [36]. The measured values for $\alpha_{\pi^\pm p}$ are also available in Ref. [36] at higher energies only. Therefore, $\alpha_{\pi^\pm p}$ has been generated at lower energies by using SAID program [37]. For π^\pm neutron scattering parameters, they are approximated as: $\alpha_{\pi^\pm n} \approx \alpha_{\pi^\mp p}$ and $\sigma_t^{\pi^\pm n} \approx \sigma_t^{\pi^\pm d} - \sigma_t^{\pi^\pm p}$. The data for the pion deuteron total scattering cross section $\sigma_t^{\pi^\pm d}$ are also available in the Ref. [36].

The rho meson, being an unstable particle, can not exist as beam. Therefore, $\alpha_{\rho^0 N}$ and $\sigma_t^{\rho^0 N}$ [which are required in Eq. (17) to estimate the ρ^0 nucleus optical potential $V_{O\rho}(\mathbf{r})$] can not be measured directly. On the other hand, they can be extracted from the ρ production data available for various elementary reactions. In fact, several authors have done this exercise recently for a wide range of ρ energy. In one of these calculations, using Vector Dominance Model (VDM) Kondratyuk et al., [21] have extracted the ρ nucleon scattering amplitude $f_{\rho N}$ from the rho meson photoproduction data at higher energies ($E_\rho \geq 2$ GeV). At lower energies ($E_\rho \leq 2$ GeV) they have calculated $f_{\rho N}$ using Resonance Model (RM), since the rho meson couples strongly to a number of resonances in this energy region. There exists another calculation, where Lutz et al., using couple channel approach [38], have calculated $f_{\rho N}$ in the region of threshold ρ production. In this energy region, their calculations reproduce the measured cross sections for various reactions, such as $\pi N \rightarrow \rho N$, $\gamma N \rightarrow \rho N$, very well.

As mentioned earlier, we calculate the energy transfer $E_p - E_{p'}$ distribution spectra for the $\pi^+ \pi^-$ emission, which arise due to the decay of the forward going ρ^0 meson in the nucleus. This rho meson is assumed to produce coherently in the (p, p') reaction on a nucleus. The coherent meson production process assures that the recoil nucleus remains in the same state as of the target nucleus. The forward propagation of the ρ^0 meson, as considered here for simplicity, imposes a constrain on the pion emission angle: $\theta_{\pi^+} = -\theta_{\pi^-}$. In these calculations, the p' emission angle is taken fixed at 1° .

For the above reaction on ^{12}C nucleus, the sensitivity of the cross section on the pion emission angle is presented in Fig. 1 at 2.5 GeV beam energy. The cross sections have been calculated for various π^+ emission angles θ_{π^+} taken sequentially from 5° to 35° . In this figure, we show the calculated results only for θ_{π^+} taken equal to 20° , 25° and 30° . This figure shows that the peak position gets shifted towards the lower value of $E_p - E_{p'}$ with the increase in the π^+ emission angle. It also shows the cross section is maximum for the π^+ emission angle taken equal to 25° . For this angle, the cross section at the peak is $82.5 \mu\text{b}/(\text{GeV}^2\text{sr}^3)$, which appears at the energy transfer $E_p - E_{p'}$ equal to 1.64 GeV. The peak cross section for θ_{π^+} taken equal to 20° is $52.35 \mu\text{b}/(\text{GeV}^2\text{sr}^3)$, appearing at $E_p - E_{p'}$ equal to 1.74 GeV. Where as, the cross section at the peak for θ_{π^+} taken at 30° is about $48 \mu\text{b}/(\text{GeV}^2\text{sr}^3)$, and

it appears at $E_p - E_{p'}$ equal to 1.43 GeV.

In nuclear reactions, it is often seen that the cross section strongly depends on the beam energy. To show this dependence, the energy transfer $E_p - E_{p'}$ distribution spectra have been calculated for the above reaction at beam energies taken equal to 2.5, 3 and 3.5 GeV. The π^+ emission angle θ_{π^+} is taken fixed at 25° , since this settings, as shown in Fig. 1, gives the maximum cross section at 2.5 GeV beam energy. The calculated $E_p - E_{p'}$ distribution spectra are presented in Fig. 2, which shows the cross section increases with the increase in beam energy. The cross section at the peak is enhanced to $0.75 \text{ mb}/(\text{GeV}^2\text{sr}^3)$ at 3.5 GeV from $82.5 \mu\text{b}/(\text{GeV}^2\text{sr}^3)$ at 2.5 GeV. The peak position at 3.5 GeV beam energy appears at $E_p - E_{p'}$ equal to 1.74 GeV, where as it appears at $E_p - E_{p'} = 1.64 \text{ GeV}$ for the beam energy taken equal to 2.5 GeV. At 3 GeV, the calculated cross section at the peak is $0.4 \text{ mb}/(\text{GeV}^2\text{sr}^3)$, and it appears at $E_p - E_{p'}$ equal to 1.7 GeV.

An unstable particle, while propagating through a nucleus, can decay inside as well as outside the nucleus, depending upon its velocity and the size of the nucleus. To explore it for ρ^0 meson propagating through the ^{12}C nucleus, the cross sections for the inside and outside decay probabilities have been compared in Fig. 3 at 3.5 GeV beam energy. The π^+ emission angle is taken equal to 20° , since it gives the maximum cross section (not shown) at 3.5 GeV beam energy. The peak cross section for the rho meson decaying inside of this nucleus is $0.12 \text{ mb}/(\text{GeV}^2\text{sr}^3)$, appearing at $E_p - E_{p'}$ equal to 1.98 GeV (dotted line). Where as it is equal to $\sim 1.46 \text{ mb}/(\text{GeV}^2\text{sr}^3)$ at $E_p - E_{p'} = 2.12 \text{ GeV}$ for ρ^0 decaying outside the same nucleus (dashed line). Therefore, the outside decay cross section for this reaction dominates by a factor about 12 over the inside decay cross section. This figure also compares the coherent and incoherent contributions to the cross section, coming from the inside and outside decay amplitudes for ρ^0 traveling through the ^{12}C nucleus. As illustrated in this figure, the peak cross section due to incoherent contribution is about $1.57 \text{ mb}/(\text{GeV}^2\text{sr}^3)$ at $E_p - E_{p'} = 2.12 \text{ GeV}$ (dash-dot line). On the other hand, it is $\sim 2.17 \text{ mb}/(\text{GeV}^2\text{sr}^3)$ due to coherent contribution, appearing at $E_p - E_{p'}$ equal to 2.08 GeV (solid line). Therefore, the coherent contribution supercedes the incoherent contribution by a factor about 1.4.

The inside decay probability for the rho meson should increase while it propagates through a larger nucleus. To show this, the cross sections for ρ^0 meson decaying inside as well as outside the ^{208}Pb nucleus have been calculated at 3.5 GeV beam energy. The π^+ emission angle is taken at 15° in this case, since it gives maximum cross section for the Pb target. The calculated results are presented in Fig. 4. It is noticeable in this figure that the peak cross sections for the inside and outside decay probabilities of the ρ^0 meson, traveling through the Pb nucleus, are comparable to each other [$\sim 65 \mu\text{b}/(\text{GeV}^2\text{sr}^3)$], unlike the case happening for ^{12}C nucleus (see in

Fig. 3). Another remarkable aspect appearing in this figure is the enhancement in the cross section due to the interference between the inside and outside decay amplitudes for the ρ^0 meson. The peak cross section due to incoherent contribution is $0.11 \text{ mb}/(\text{GeV}^2\text{sr}^3)$ at $E_p - E_{p'}$ equal to 2.2 GeV (dash-dot). Where as, it is equal to $0.22 \text{ mb}/(\text{GeV}^2\text{sr}^3)$ due to coherent contribution, appearing at $E_p - E_{p'} = 2.19 \text{ GeV}$ (solid line). Therefore, the interference effect enhances the cross section over the incoherent contribution by a factor of 2 for the Pb nucleus, which is significantly larger than that for the C nucleus.

It is always very interesting to investigate the initial and final state interactions in the nuclear reactions. The effect of these interactions on the $\pi^+\pi^-$ emission in the (p, p') reaction on ^{12}C nucleus is shown in Fig. 5 at 3.5 GeV beam energy. This figure compares the calculated distorted wave results for the continuum particles (i.e., p , p' , π^+ and π^-) with the plane waves results. In addition, the nuclear effect on the ρ propagation through the ^{12}C nucleus is also presented. The plane wave result (which also includes the free ρ^0 propagator) shows the cross section is $25.54 \text{ mb}/(\text{GeV}^2\text{sr}^3)$ at the peak, appearing at $E_p - E_{p'}$ equal to 2.02 GeV (dash-dot-dot line). The distortion due to projectile proton p brings down the peak cross section to $7.02 \text{ mb}/(\text{GeV}^2\text{sr}^3)$ at $E_p - E_{p'} = 2.04 \text{ GeV}$ (dash-dot line). Therefore, the initial state interaction reduces cross section by a factor about 3.64 at the peak, and it shifts the peak position by 20 MeV towards the higher side in the $E_p - E_{p'}$ distribution spectrum. The incorporation of the distortion due to ejectile proton p' further attenuates the peak cross section to $2.6 \text{ mb}/(\text{GeV}^2\text{sr}^3)$ at $E_p - E_{p'} = 2.05 \text{ GeV}$ (dashed line). Therefore, the projectile and ejectile (i.e., p and p') distortions together reduce the plane wave cross section by a factor about 9.82 at the peak, and they shift the peak position by 30 MeV towards the higher value of $E_p - E_{p'}$. The final state interactions due to $\pi^+\pi^-$ together shift the peak position to $E_p - E_{p'} = 2.07 \text{ GeV}$, leaving the magnitude of the peak cross section [$\sim 2.38 \text{ mb}/(\text{GeV}^2\text{sr}^3)$] almost unaffected (dotted line). Therefore, the overall final state interactions reduce the cross section by a factor about 2.95 at the peak, and they shift the peak position by 30 MeV towards the higher side in the $E_p - E_{p'}$ distribution spectrum. The initial and final state interactions together, as shown in this figure, bring down the plane wave cross section by a factor ~ 10.7 at the peak, and they also shift the peak position by 50 MeV towards the higher value in the $E_p - E_{p'}$ distribution spectrum. The ρ^0 nucleus interaction (which appears in the rho meson propagator) is found not much sensitive to the cross section. It attenuates the peak cross section only by about 8.8%, i.e., from $2.38 \text{ mb}/(\text{GeV}^2\text{sr}^3)$ to $2.17 \text{ mb}/(\text{GeV}^2\text{sr}^3)$, and it shifts the peak position by 10 MeV to $E_p - E_{p'} = 2.08 \text{ GeV}$ (solid line).

The initial and final state interactions could be very intensive for those nuclear reactions, which involve heavier nuclei. To illustrate it, the calculated plane and

distorted wave results for the Pb nucleus are presented in Fig. 6. As exhibited in this figure, the plane wave results (which also incorporates the free ρ^0 propagator) show oscillations in the energy transfer $E_p - E_{p'}$ spectrum (dash-dot-dot line). It arises due to the oscillatory nature of the form factor for the Pb nucleus. The initial state interaction reduces this oscillation drastically, showing a prominent peak at 2.01 GeV in the energy transfer $E_p - E_{p'}$ spectrum (dash-dot line). The cross section at this peak is about 0.74 (mb/GeV²sr³). Therefore, the initial state interaction alone brings down the cross section at the main peak by a factor about 179, and it shifts the peak position by 50 MeV towards the lower value of $E_p - E_{p'}$. The incorporation of p' distortion reduces the peak cross section further to 0.35 mb/(GeV²sr³), at $E_p - E_{p'}$ equal to 2.07 GeV (dashed line). Therefore, the projectile and ejectile (i.e., p and p') distortions together attenuate the cross section at the main peak by a factor about 379, and it shifts the peak position by 10 MeV only towards the higher side in the $E_p - E_{p'}$ distribution spectrum. The final state interactions due to $\pi^+\pi^-$ together flatten the peak considerably, and they further reduce the peak cross section to ~ 0.25 mb/(GeV²sr³) (dotted line). Therefore, the final state interactions altogether bring down the cross section by a factor about 3. In this case, the ρ nucleus interaction reduces the cross section 12%, i.e., from 0.25 mb/(GeV²sr³) to 0.22 mb/(GeV²sr³), leaving the shape for the spectrum unchanged (solid line).

4 Conclusion

This study shows that the cross section for the $\pi^+\pi^-$ emission from the forward going coherent ρ^0 meson, produced in the (p, p') reaction, reaches its maximum value for a certain direction of the pion emission. The cross section strongly depends on the beam energy. The probability for the rho meson decaying inside the nucleus is less for lighter nucleus. It increases with the size of the nucleus. However, the interference between the inside and outside decay amplitudes for the rho meson is very important in evaluating the cross section. The initial and final state interactions significantly dampen the plane wave cross section, which is drastic for the heavier nucleus.

5 Acknowledgement

I gratefully acknowledge Dr. A.K. Mohanty for his encouragement.

References

- [1] A. Drees, Nucl. Phys. **A610**, 536c (1996); CERES Collaboration, Th. Ullrich, Nucl. Phys. **A610**, 317c (1996); HELIOS-3 Collaboration, M. Masera, Nucl. Phys. **A590**, 93c (1995); NA50 Collaboration, E. Scomparin, Nucl. Phys. **A610**, 331c (1996).
- [2] G.Q. Li, C.M. Ko and G.E. Brown, Phys. Rev. Lett. **75**, 4007 (1995); G.Q. Li, C.M. Ko, G.E. Brown and H. Sorge, Nucl. Phys. **A611**, 539 (1996); W. Cassing, W. Ehehalt and C.M. Ko, Phys. Lett. **B363**, 35 (1995); W. Cassing, W. Ehehalt and I. Kralik, Phys. Lett. **B377**, 5 (1996).
- [3] G. Chanfray, R. Rapp and J. Wambach, Phys. Rev. Lett. **76**, 368 (1996); R. Rapp, G. Chanfray and J. Wambach, Nucl. Phys. **A617**, 472 (1997); W. Cassing, E.L. Bratkovskaya, R. Rapp and J. Wambach, Phys. Rev. C **57**, 916 (1998); R. Rapp and J. Wambach, Eur. Phys. J. **A6**, 415 (1999).
- [4] J. Adams et al., Phys. Rev. Lett. **92**, 092301 (2004).
- [5] G.E. Brown and M. Rho, Phys. Rev. Lett. **66**, 2720 (1991).
- [6] T. Hatsuda and S.H. Lee, Phys. Rev. C **46**, R34 (1992).
- [7] M. Asakawa, C.M. Ko, P. Lévai and X.J. Qiu, Phys. Rev. C **46**, R1159 (1992); M. Asakawa and C.M. Ko, Phys. Rev. C **48**, R526 (1993); Nucl. Phys. **A560**, 399 (1993).
- [8] K. Saito, K. Tsushima and A.W. Thomas, Phys. Rev. C **55**, 2637 (1997); **56**, 566 (1997).
- [9] B. Friman, Nucl. Phys. **A610**, 358c (1996); B. Friman and H.J. Pirner, Nucl. Phys. **A617**, 496 (1997).
- [10] W. Peters, M. Post, H. Lenske, S. Leupold and U. Mosel, Nucl. Phys. **A632**, 109 (1998); M. Post, S. Leupold and U. Mosel, Nucl. Phys. **A689**, 753 (2001).
- [11] M. Herrmann, B.L. Friman and W. Nörenberg, Z. Phys. **A343**, 119 (1992); Nucl. Phys. **A560**, 411 (1993).
- [12] C.M. Ko, V. Koch and G. Li, Annu. Rev. Nucl. Part. Sci. **47**, 505 (1997); W. Cassing and E.L. Bratkovskaya, Phys. Rep. **308**, 65 (1999); R. Rapp and J. Wambach, Adv. Nucl. Phys. **25**, 1 (2000).

- [13] “Nuclear mass dependence of vector meson using the photoproduction of lepton pairs”, CEBAF proposal PR 89-001, Spokesperson: D. Heddle and B.M. Preedom (unpublished); “Photoproduction of vector meson off nuclei”, CEBAF Proposal PR 94-002, Spokesmen: P.Y. Bertin, M. Kossov and B.M. Preedom (unpublished).
- [14] “Current Experiments in Elementary Particle Physics”, Report Nos. INS-ES-134 and INS-ES-144, Report No. LBL-91 revised, UC-414, 1994 p.108 (unpublished); K. Maruyama, Proceedings of the 25th International Symposium on Nuclear and Particle Physics with High Intensity Proton Accelerators (World Scientific, Singapore, 1998; Nucl. Phys. **A629**, 351c (1998).
- [15] CBELSA/TAPS Collaboration, D. Trnka et al., Phys. Rev. Lett. **94**, 192303 (2005).
- [16] R. Muto et al., J. Phys. G: Nucl. Part. Phys. **30**, S1023 (2004).
- [17] H. En’yo et al., KEK Experiment E325; S. Yokkaichi et al., KEK-PS E325 Collaboration, Nucl. Phys. **A638**, 435c (1998).
- [18] HADE Collaboration, W. Koenig, in Proceedings of the Workshop on Dilepton Production in Relativistic Heavy Ion Collisions, edited by H. Bokemeyer (GSI, Darmstadt, 1994), p.225; HADE Proposal, R. Schicker et al., Nucl. Instr. Meth. **A380**, 586 (1996); J. Friese, Prog. Part. Nucl. Phys. **42**, 235 (1999).
- [19] M. Fujiwara, Prog. Part. Nucl. Phys. **50**, 487 (2003).
- [20] V.L. Eletsky and B.L. Ioffe, Phys. Rev. Lett. **78**, 1010 (1997); V.L. Eletsky, B.L. Ioffe and J.I. Kapusta, Eur. Phys. J. **A3**, 381 (1998).
- [21] L.A. Kondratyuk, A. Sibirtsev, W. Cassing, Ye.S. Golubeva and M. Effenberger, Phys. Rev. C **58**, 1078 (1998).
- [22] M. Effenberger, E.L. Bratkovskaya, and U. Mosel, Phys. Rev. C **60**, 044614 (1999).
- [23] Th. Weidmann, E.L. Bratkovskaya, W. Cassing and U. Mosel, Phys. Rev. C **59**, 919 (1999); M. Effenberger, E.L. Bratkovskaya, W. Cassing and U. Mosel, Phys. Rev. C **60**, 027601 (1999).
- [24] Ye.S. Golubeva, L.A. Kondratyuk and W. Cassing, Nucl. Phys. A **625**, 832 (1997).

- [25] D. Cabrera and M.J. Vicente Vacas, Phys. Rev. C **67**, 045203 (2003); D. Cabrera, L. Roca, E. Oset, H. Toki and M.J. Vicente Vacas, Nucl. Phys. A **733**, 130 (2004); V.K. Magas, L. Roca and E. Oset, nucl-th/0403067.
- [26] T. Ericson and W. Weise, Pions and Nuclei (Clarendon Press, Oxford, 1988).
- [27] E. Oset, H. Toki and W. Weise, Phys. Rep. **83**, 281 (1982); C. Gaarde, Annu. Rev. Nucl. Part. Sci. **41**, 187 (1991).
- [28] I. Laktineh, W.M. Alberico, J. Delorme and M. Ericson, Nucl. Phys. **A555**, 237 (1993); R.C. Carrasco, J. Nieves and E. Oset, Nucl. Phys. **A565**, 797 (1993); B. Krusche et al., Phys. Lett. **B526**, 287 (2002); D. Drechel, L. Tiator, S.S. Kamalov and S.N. Yang, Nucl. Phys. **A660**, 423 (1999); R.J. Loucks and V.R. Pandharipande, Phys. Rev. C **54**, 32 (1996); M.J.M. van Sambeek et al., Nucl. Phys. **A631**, 545c (1998).
- [29] J. Chiba et al., Phys. Rev. Lett. **67**, 1982 (1991); T. Hennino et al., Phys. Lett. **B303**, 236 (1993).
- [30] V.F. Dmitriev, Phys. Rev. C **48**, 357 (1993); P. Oltmanns, F. Osterfeld and T. Udagawa, Phys. Lett. **B299**, 194 (1993); F. Osterfeld, B. Körfgen, P. Oltmanns and T. Udagawa, Phys. Scr. **48**, 95 (1993); T. Udagawa, P. Oltmanns, F. Osterfeld and S.W. Hong, Phys. Rev. C **49**, 3162 (1994); B. Körfgen, F. Osterfeld and T. Udagawa, Phys. Rev. C **50**, 1637 (1994); P.F. de Córdoba, J. Nieves, E. Oset and M.J. Vicente-Vacas, Phys. Lett. **B319**, 416 (1993); E. Oset, P.F. de Córdoba, J. Nieves and M.J. Vicente-Vacas, Phys. Scr. **48**, 101 (1993); P.F. de Córdoba, E. Oset and M.J. Vicente-Vacas, Nucl. Phys. **A592**, 472 (1995).
- [31] R. Machleidt, Adv. Nucl. Phys. **19**, 189 (1989).
- [32] R.K. Bhaduri, Models of the Nucleon (Addison-Wesley Publishing Company, Inc., 1988).
- [33] Swapan Das, Phys. Rev. C **70**, 034604 (2004); B.K. Jain and Bijoy Kundu, Phys. Rev. C **53**, 1917 (1996).
- [34] H.De. Vries and C.W. De Jager, Atomic data and Nuclear data tables **14**, 479 (1974).
- [35] D.V. Bugg et al., Phys. Rev. C **146**, 980 (1966); S. Barshay et al., Phys. Rev. C **11**, 360 (1975); W. Grein, Nucl. Phys. B **131**, 255 (1977); C. Lechanoine-LeLue, Rev. Mod. Phys. **65**, 47 (1993).

- [36] Particle Data Group, Phys. Rev. C **54**, 192-195 (1996).
- [37] R.A. Arndt et al., SAID Programme (URL: <http://gwdac.phys.gwu.edu>).
- [38] M.F.M. Lutz, Gy. Wolf and B. Friman, Nucl. Phys. A **706**, 431 (2002).

Figure Captions

1. The sensitivity of the energy transfer $E_p - E_{p'}$ distribution spectrum on the pion emission angle is shown in this figure. The peak cross section is maximum for the π^+ emission angle taken equal to 25° . The peak position gets shifted towards the lower value of $E_p - E_{p'}$ with the increase in the pion emission angle.
2. The dependence of the energy transfer $E_p - E_{p'}$ distribution spectrum on the beam energy is presented here. With the increase in the beam energy, the cross section increases and the peak position moves towards the higher value of $E_p - E_{p'}$. The π^+ emission angle is taken fixed at 25° (see text).
3. The cross sections for the rho meson decaying inside and outside the nucleus are compared for ^{12}C nucleus at 3.5 GeV beam energy. The outside decay cross section superceeds for this nucleus. The interference between the inside and outside decay amplitudes enhances the cross section. Various lines are explained in the text.
4. The inside and outside decay cross sections are shown for the rho meson propagating through the ^{208}Pb nucleus. The inside decay cross section is substantially increased for the heavier nucleus. In this case, the interference due to the ρ^0 inside and outside decay amplitudes is more stronger than that for the ^{12}C nucleus.
5. The effect of the initial and final state interactions on the cross section, for the $(p, p'[\pi^+\pi^-])$ reaction on the ^{12}C nucleus, is illustrated here. The beam energy is taken equal to 3.5 GeV. The nuclear effect on the ρ propagation is also presented. Various lines have been described in the text.
6. The initial and final state interactions arising due to ^{208}Pb nucleus are exhibited in this figure. Compare to ^{12}C nucleus, these interactions are more intense for the Pb nucleus. Various lines are defined in the text.

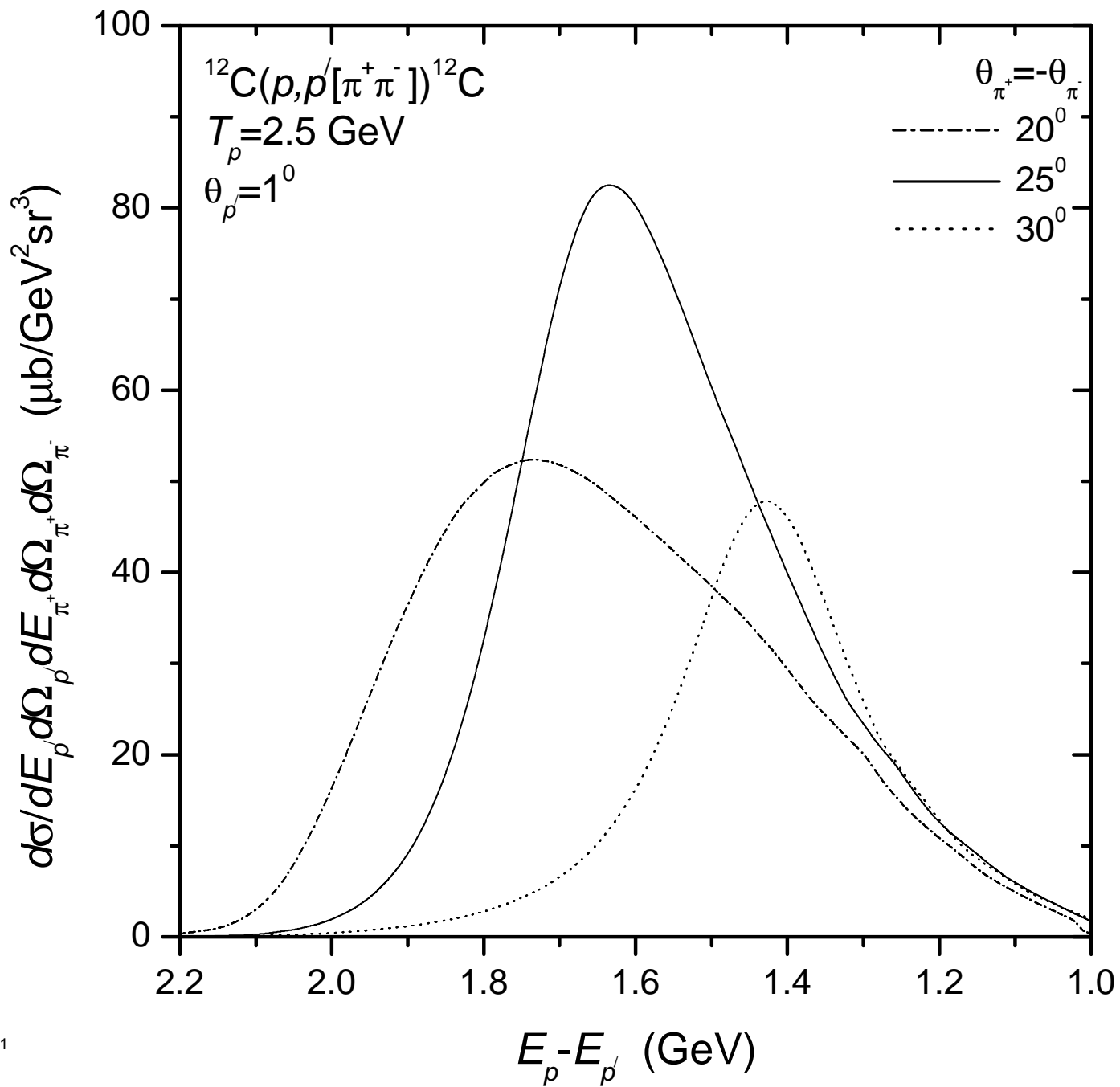


Fig. 1

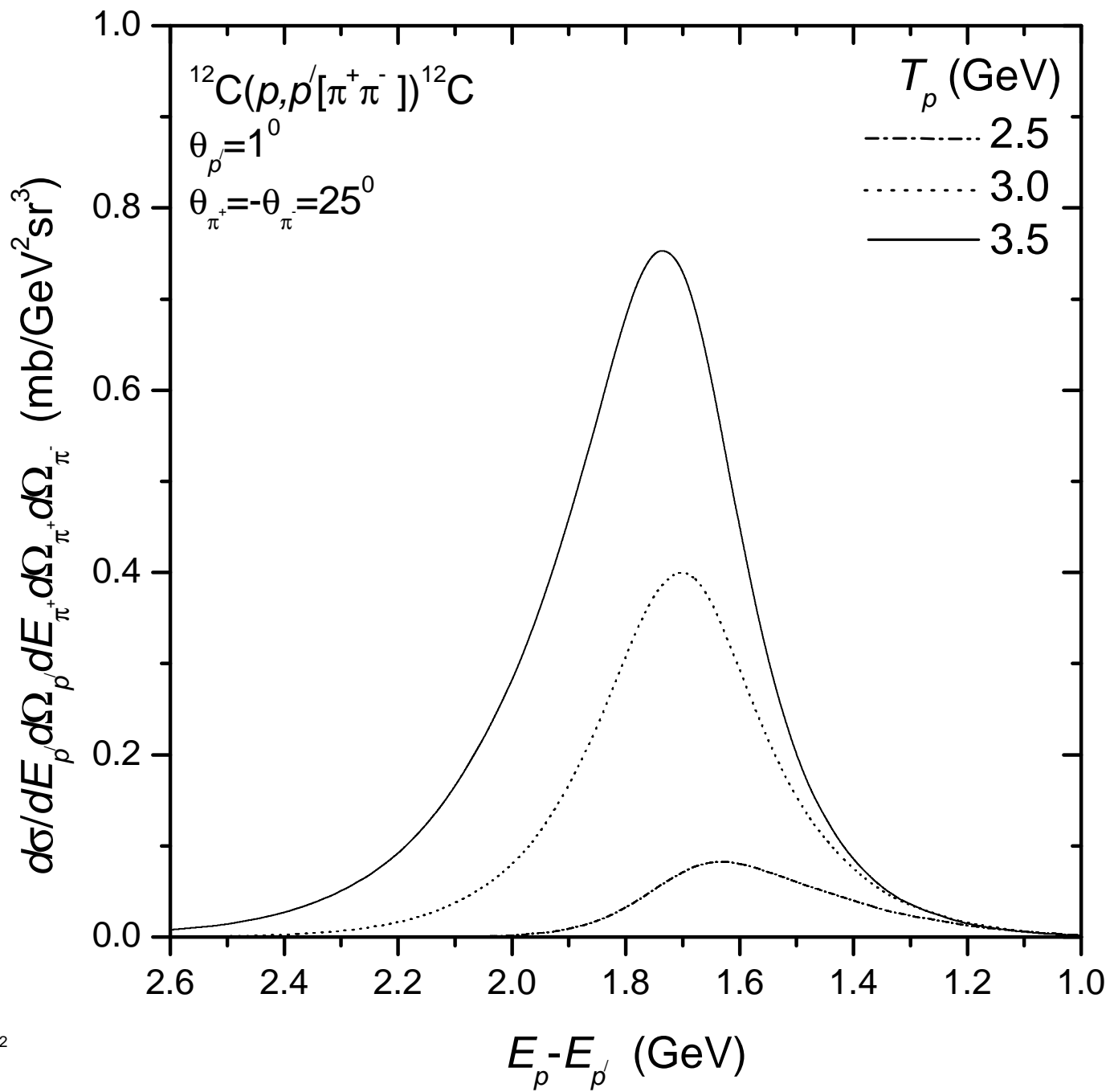


Fig. 2

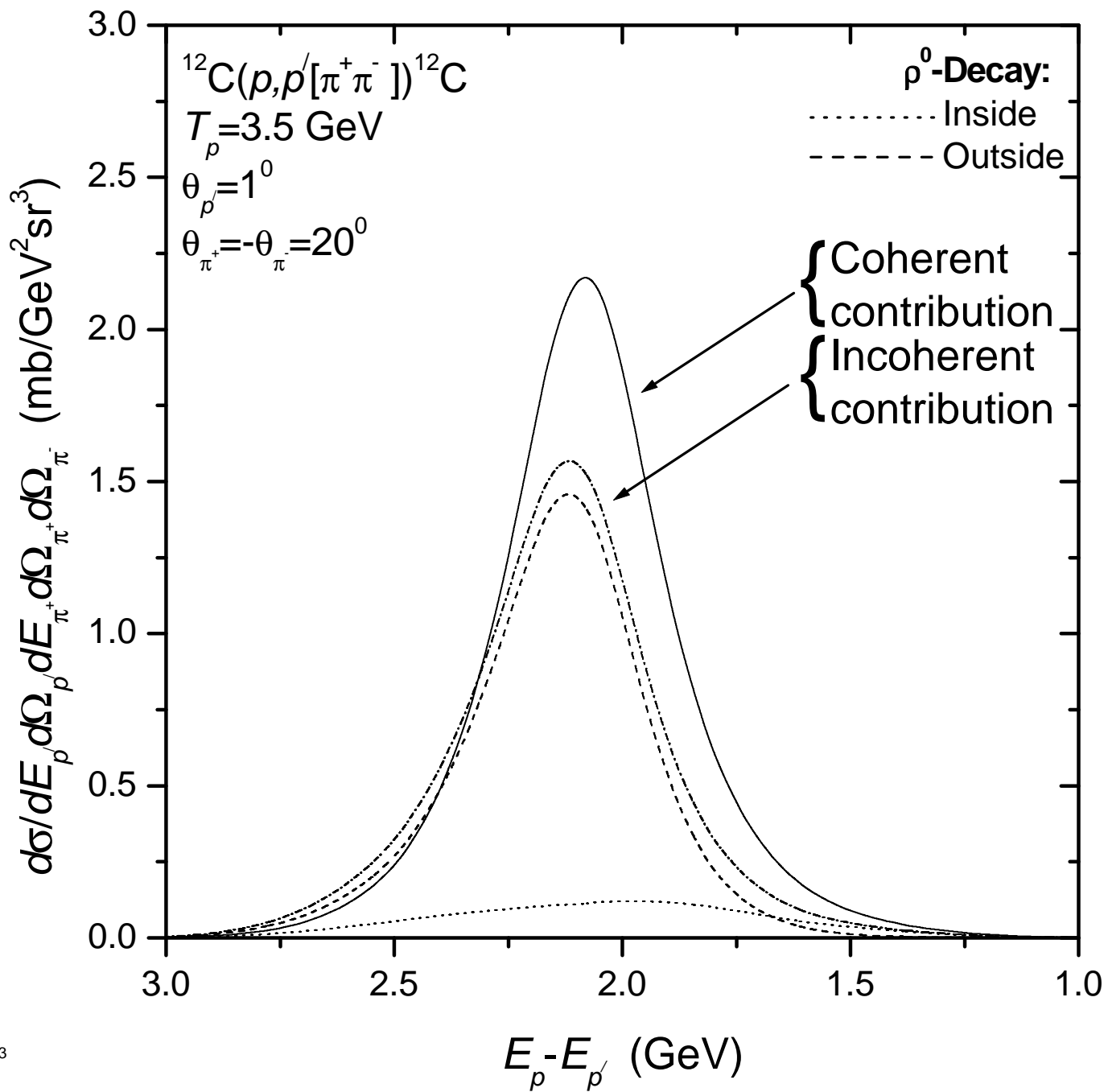


Fig. 3

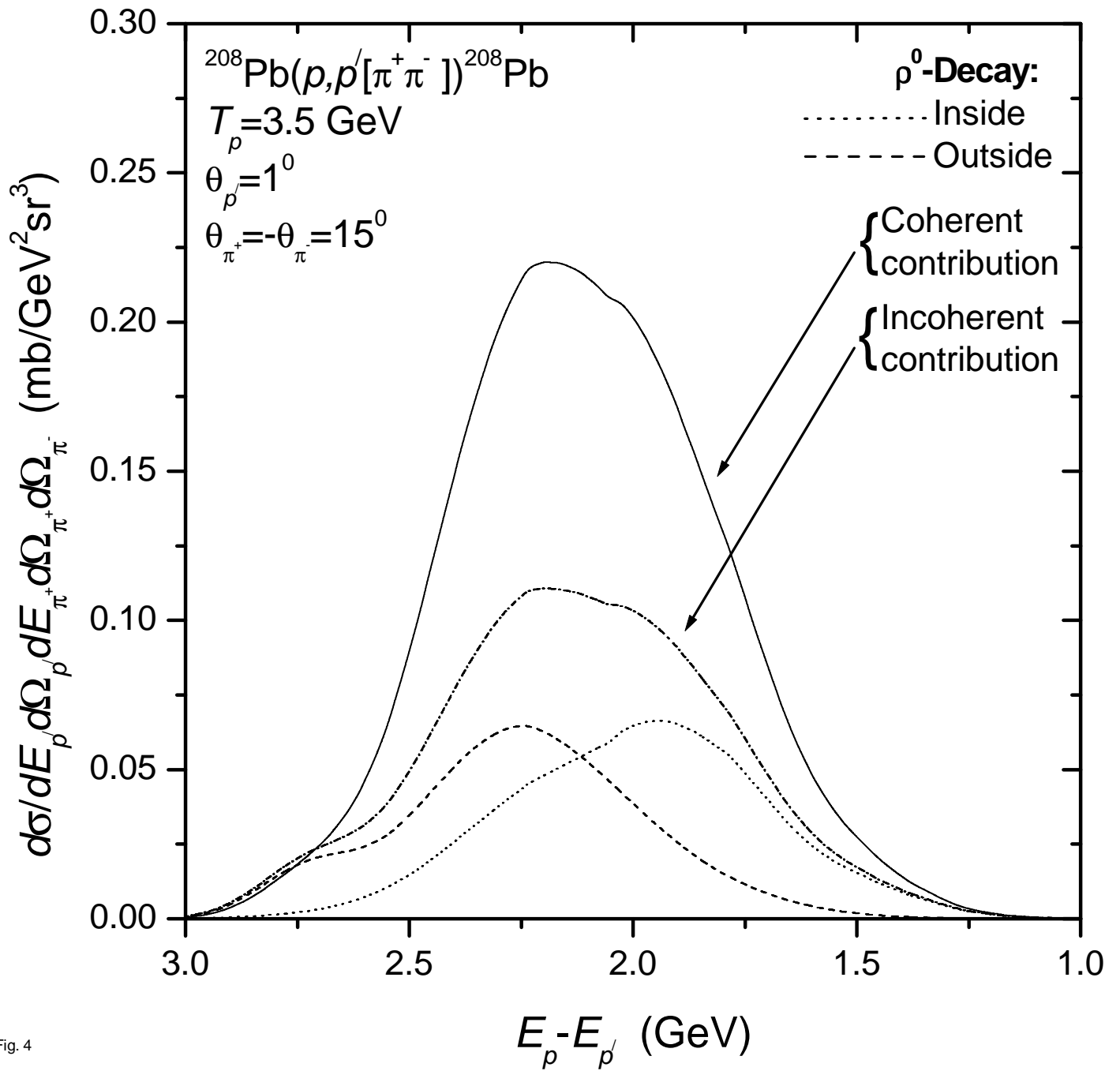


Fig. 4

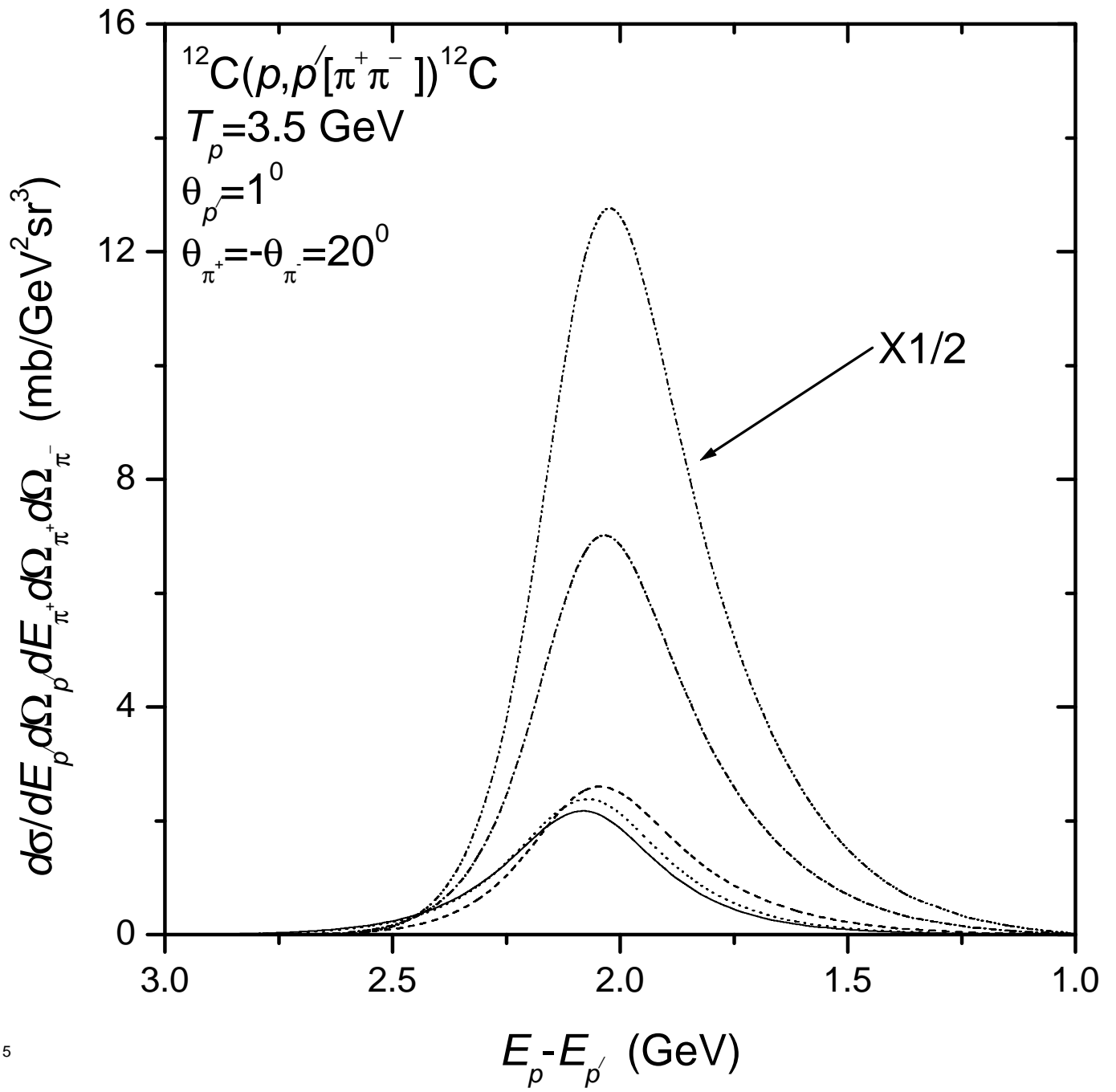


Fig. 5

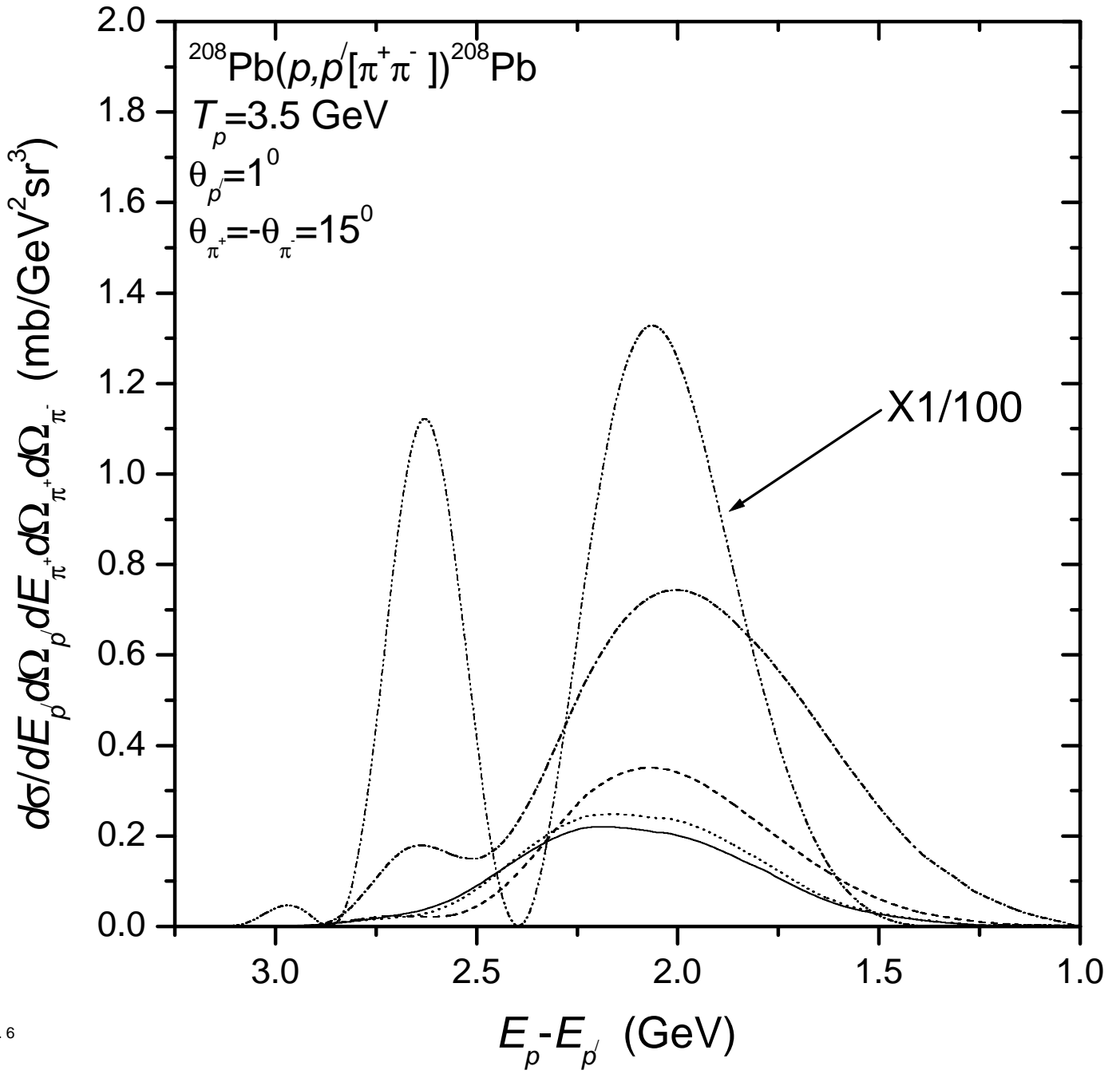


Fig. 6